Multi-objective Optimized Smart Charge Controller for Electric Vehicle Applications

Zunaib Ali, Ghanim Putrus, Mousa Marzband, *Senior Member, IEEE,* Hamid Reza Gholinejad, *Student Member, IEEE,* Komal Saleem, *Student Member, IEEE,* and Bidyadhar Subudhi, *Senior Member, IEEE*

***Abstract*—The continuous deployment of distributed energy sources and increase in the adoption of Electric Vehicles (EVs) require smart charging algorithms. Existing EV chargers offer limited flexibility and controllability, and do not fully consider factors (such as, EV user waiting time and length of next trip) as well as the potential opportunities and financial benefits from using EVs to support the grid, charge from renewable energy and deal with the negative impacts of intermittent renewable generation. The lack of adequate smart EV charging may result in high battery degradation, violation of grid control statutory limits, high greenhouse emissions and charging cost. In this paper, a Neuro-Fuzzy-PSO based novel and advanced smart charge controller is proposed which considers user requirements, energy tariff, grid condition (e.g., voltage or frequency), renewable (PV) output and battery state of health. A rule based Fuzzy controller becomes complex as the number of inputs to the controller increases. Also, it becomes difficult to achieve an optimum operation due to conflicting nature of control requirements. To optimize the controller response, Particle Swarm Optimization (PSO) technique is proposed to provide a global optimum solution based on a pre-defined cost function and to address the implementation complexity PSO is combined with neural network. The proposed Neuro-Fuzzy-PSO control algorithm meets EV user requirements, work within technical constraints and is simple to implement in real-time (and requires less processing time). Simulation using MATLAB and experimental results using dSPACE digital real-time emulator are presented to demonstrate the effectiveness of the proposed controller.**

***Index Terms*—Electric vehicle, smart charge controller, Fuzzy logic, neural network, battery health, smart power networks**

I. Introduction

THE increasing integration of distributed Renewable Energy Resources (RES) and Electric Vehicles (EVs) (aiming to reduce carbon footprints as well as support sustainable energy and transport [1]–[3]) necessitates smart and dynamic power system control in order for network to stay within the statutory limits (e.g. voltage and frequency thresholds) and avoid overloading of equipment (e.g. feeders, transformers etc.) [4], [5]. Further, it is important for the user to consider the energy tariff (which varies on hourly basis) to get maximum financial benefits, such as charging EVs during periods of surplus generation, especially from RES. Moreover, as the battery is the most expensive part of an EV, attention should be given to extending battery life [6] and reduce the overall cost of ownership of the EV. The continuous increase in the deployment of EVs (as well as RES) and the efforts to achieve 2050 climate targets may be hindered due to lack of smart charging infrastructures and advanced battery technology. From the control aspect, there is an essential requirement for efficient, reliable and simple (less-complex) to implement EV smart chargers that can provide similar driver-experience to conventional vehicle-refueling framework. An ideal smart charge controller should be able to: (a) meet EV user requirements, (b) support the grid, (c) deal with intermittent nature of renewables, (d) charge EV from renewable energy, (e) increase energy autonomy and (f) do these with minimum degradation to the EV battery. Thus, there is a need to develop a smart EV charge controller that can meet as many of these attributes. Thus there is a need to develop an intelligent control algorithm which provides optimized response and lower complexity [7]. The interaction of the smart controller with the EV user and network is depicted in Fig. 1.

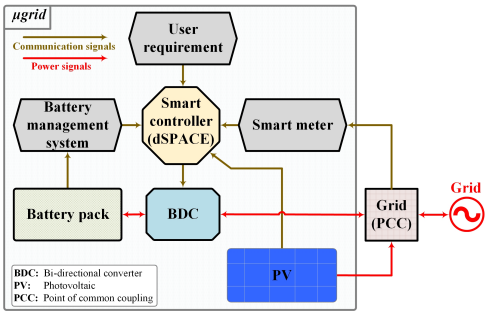

Fig. 1. Smart charge controller interface links.

Research into EV smart charging aims to develop optimum charging algorithms to meet EV user requirements whilst reducing the negative impact of charging on the electricity grid as well as minimizing charging time and battery degradation. Several studies [8]–[12] investigated the impact of residential EV charging on the grid and discussed how to minimize its impact on the grid demand. Charging techniques to mitigate the effect of grid voltage sag and improving steady-state voltage stability is presented in [13], [14], where a centralized aggregator manages EV chargers by collecting the information such as charging time, departure and arrival of EVs from various charging points in the network. The aggregator controls the charging commands in response to

Manuscript received May xx, 2021. The work is supported by the British Council under grant contract No: IND/CONT/GA/18-19/22 and Innovatve UK grant number 10004690.

Z. Ali and K. Saleem are with London Center of Energy Engineering (LCEE), School of Engineering, London South Bank University, London, United Kingdom (e-mails: aliz29@lsbu.ac.uk and saleemk2@lsbu.ac.uk).

G. Putrus is with Faculty of Engineering and Environment, Department of Mathematics, Physics and Electrical Engineering, University of Northumbria, Newcastle, United Kingdom (e-mail: ghanim.putrus@northumbria.ac.uk).

Mousa Marzband is with Faculty of Engineering and Environment, Department of Maths,Physics and Electrical Engineering, University of Northumbria, Newcastle, United Kingdom and also with the center of research excellence in renewable energy and power systems, King Abdulaziz University, Jeddah, Saudi Arabia (e-mail:mousa.marzband@northumbria.ac.uk)

H. R. Gholinejad is with the Department of Electrical and Computer Engineering, Babol University of Technology, Babol, Iran.

B. Subudhi is with the School of Electrical Sciences, Indian Institute of Technology, Goa, India.

network conditions determined by a power flow analysis carried out every 5 mins. The method however is not dynamic to respond to instantaneous changes in the system, especially to stochastically varying RES generation and EV charging. In addition, this centralized approach may not meet the individual EV users' needs and charging profiles.

A differential pricing scheme described in [15] offers reduced tariffs during grid low power demand, encouraging users to charge during such periods and prevent charging at time of peak load. Thus, reducing the potential overloading of the grid or voltage dips during charging. The impact of EV charging on the distribution network voltage is investigated in [16] where the arrival and departure times, and initial State of Charge (SOC) of EVs are considered for determining the charging current. The user requirements are not considered and it is assumed that the EV is charged to its maximum capacity with no consideration to battery degradation. The analysis shows a reduction in the grid voltage below the minimum statutory limit during peak hours of EV interconnection. An aggregator based intelligent automatic scheduling of EV charging is presented in [17] for mitigating load variations and low load factor. The decision is made based on charging requirements, arrival and departure times, and a voltage level is set for charging to control the demand profile. Based on certain EV requirements, a fixed charge rate is generated without considering the impact of tariff, battery degradation and voltage variations. EV smart charging presented in [18]–[20] consider system cost (including EV energy) and primarily focuses on mitigating the negative effect of peak demand, whereas the user requirements, battery degradation and utilization of RES is not considered.

A centralized controller managing the charging of Plug-in EVs has been discussed in [21] where fixed charging rate is used together with on-load tap changer and capacitor switching to achieve grid support and customer satisfaction. The main consideration is to minimize daily power loss and voltage deviation while maximizing user satisfaction. A fuzzy based decentralized real-time EV charging controller is suggested in [22] for Vehicle to Grid (V2G) services. 50% of total EV battery capacity is reserved for driving purpose, whereas the remaining provides auxiliary services to the grid (such as voltage and frequency support). The controller, however, does not consider the health of battery (such as aging/degradation) and user requirements are not satisfied. An interesting solution of optimal control of EV charging station is presented in [23] for reducing the negative impact of EV charging on grid. A method proposed in [24] provides saving to customers and avoids extra peak demands by continuously monitoring electricity prices and accordingly switching EV batteries. However, utilization of renewables towards increasing financial profit, influence of charging on battery health and user requirements are not considered. A Fuzzy controller has been suggested in [25] for EV charging that consider user needs, battery degradation and provide grid support, however, fails to consider the varying grid tariff and charging from RES. In addition, the algorithm is not optimized and is computationally inefficient for increased number of inputs. A recent technique [26] utilizes EV for peer-to-peer energy trading for grid support utilizing the storage of EVs and also, incorporates user preferences to further enhance EV scheduling; thus increasing profit and offsetting charging cost. However, the condition of battery state of health and the impact on low-carbon RES are not considered. The authors in [27] suggests the use of renewable energy (PV and wind) for charging EVs via an extra storage battery. The charging strategy first consumes available power from renewables and then switch to the main grid. However, it does not consider user requirements and only offer fixed charging intervals. Furthermore, the negative impacts of charging on grid and EV battery are also not considered. A price-based charging method is presented in [28], [29] which shifts charging of EV users to off-peak and help benefiting the grid avoiding peak demands and, likewise to the user by charging at low tariffs. This method does not account for user requirements, renewable availability, and battery state of health. Interesting method called random-in-window is discussed in [30], [31] which automatically adjust the charging rate based on the peak household loads and help reducing the detrimental effects on grid (e.g., transformer aging). In [32], [33], authors manage the EV charging by designing optimization algorithms aim at assigning suitable charging locations to the EV to help reduce the cost incurred by stations. This method provides grid support by EV scheduling but lacks in considering other factors. The authors in [34] presents adaptive charging network (ACN) which considers request from users and information from grid for trigging the charging events. The impact of charging on EV SOH and the contribution of renewables towards charging are though not considered. This demonstrate the need for a decentralized controller that meets user requirements, grid preferences, sustainable energy and battery health. A detailed comparison of existing techniques with the proposed controller is summarized in Table I.

In this paper, a Neuro-Fuzzy based novel and advanced smart charge controller is proposed taking into account user requirements (length of next trip and waiting time), grid information (voltage or frequency and tariff), RES (PV) power generation and battery state-of-health (SOH). A simple Fuzzy controller is initially designed, which however, becomes complex in terms of implementation as inputs to the controller increase. To reduce the complexity and simplify implementation, a Neuro-Fuzzy controller is proposed which results in a significant reduction in the number of Fuzzy rules; thus easier to implement. To optimize the controller response, for different input control variables, Particle Swarm Optimization (PSO) technique is proposed to provide a global optimum solution, based on a pre-defined specific cost function. The performance of the proposed controllers is analyzed, using simulation and experimental work, based on number of rules, complexity and performance indices (such as mean square error, mean absolute error etc.). The major contributions of this paper may be summarized as follows:

1) Comprehensively reviewed and benchmarked existing smart charge controllers, Table I.
2) Proposed a novel Neuro-optimization-based scheme to manage and achieve pre-defined EV user objectives and

TABLE I
COMPARISON OF PROPOSED CONTROLLER WITH TECHNIQUES FROM THE EXISTING LITERATURE.

Controller	Objectives						
	Individual EV user requirements	EV battery life extension	Renewable energy utilization	Microgrid/ network support	Profit/cost of energy exchanged	Dynamic tariff	Key features
[8], [11], [12]	×	×	×	✓	×	×	EV impact on load demand and remedies
[13], [14]	×	×	×	✓*	×	×	Centralized aggregator for EV charging
[15]	×	×	×	✓	×	✓	Differential pricing to shape load curve
[16]	×	×	×	✓	×	×	EV impact on voltage profile during peak hours
[17]	×	×	×	✓	×	×	Fixed charging rate and demand side load profile enhancement
[18], [20]	×	×	×	✓	✓	×	Mitigating peak load and consider EV cost
[21]	×	×	×	✓	×	×	Fixed charging rate and on-load tap changer for grid support
[22]	×	×	×	✓	×	×	50% reserved for driving and 50% for grid support
[23]	×	×	×	✓	✓	×	Optimal positioning of charging stations and reducing negative impact of EV charging
[24]	×	×	×	✓	✓	✓	Price monitoring for customer support
[25]	✓	✓	×	✓	×	×	Grid support, variable charging rate and user satisfaction
[26]	✓	×	×	✓	✓	✓	Peer to peer energy trading and tariff impact
Proposed work	✓	✓	✓	✓	✓	✓	Less complex, optimized, user-, eco- and grid- friendly

grid preferences with simple implementation.

3) Design a suitable objective function related to EV *C-rate* and profit to ensure optimization convergence.
4) Developed a real-time control platform for EV charging that uses data from the the EV user (e.g. user journey requirements), battery (capacity, state of charge and health), grid (voltage and tariff), charger power rating in order to determine the charging rate and manage the charging session.
5) Developed a Simulink model for the system and use this to design and optimize the controller parameters in simulation environment and in real-time.
6) Developed performance indices to evaluate the effectiveness of controller in terms of: (1) deviation of the actual SOC from the target value (measured as MSE), (2) implementation complexity for real-time applications (measured as number of rules and processing time), and (3) user satisfaction in terms of maximizing charging rate (reduced charging time) and financial benefits.
7) Implemented and validated the controller performance using realistic grid conditions, PV and tariff profiles as well as for various objective functions.

The rest of paper is organized as follows: Section II presents system configuration and implementation. The proposed smart charge controller is introduced in Section III. Section IV presents simulation and experimental results.

II. SYSTEM CONFIGURATION AND IMPLEMENTATION METHODOLOGY

The security and stability of grid is very important and thus, the negative impacts of increasing electric vehicles on the grid must be considered. This is achieved by making EV charging controlled and adaptable to provide active grid support rather than uncontrolled charging. Smart charge controller allows fulfilling EV user requirements with minimum impact on grid and EV itself by effectively controlling the charging current. Consequently, this paper considers grid voltage, tariff and PV penetration as control variables and provide grid support by providing variable and smart charging.

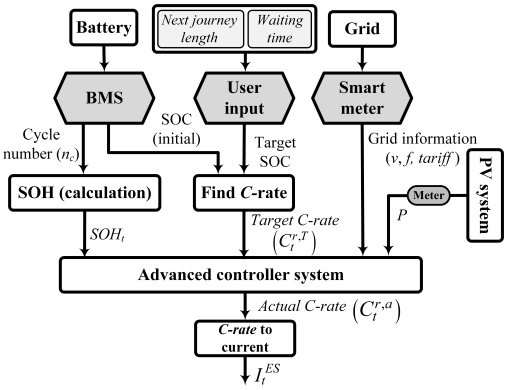

Fig. 2. Block diagram of the smart charge controller.

In essence, controller determines the charging reference signal which controls the actual charging rate $C_t^{r,a}$ considering real-time measurements from BMS, grid, RES and user inputs. Thereafter, a controllable power electronic converter enables the flow of commanded current (I_t^{ES}), as shown in Fig. 2. The factors considered by the control unit are:

a) *User requirements:* The user provides information about length of stay (waiting time) and length of

next journey. Based on that, a target SOC is set and together with measured SOC, target *C-rate* is determined.

b) *EV Battery SOC and SOH based on information from BMS:* The battery SOH and SOC is obtained from the on-board battery management system.

c) *PV system measurements:* Output power from photovoltaic system is measured.

d) *Grid information (including grid voltage conditions, frequency, tariff etc.):* The lower and upper grid voltage limits are defined in order to staying within assigned grid limits, such as for UK $400/230\,\mathrm{V}$ these limits are $0.94\,\mathrm{p.u.}$ (min) and $1.1\,\mathrm{p.u.}$ (max). Alongside, tariff data is obtained so as to support grid during period of peak demand or based on specific tariff profiting EV user.

The concept for the implementation of smart controller is given in Fig. 3. The inputs signals are derived from the user requirements, grid information, battery management system and PV generation.

A. User information

The EV user defines requirements such as length of next journey (target miles) and waiting time. The former is translated to the target SOC (SOC_t^T) using miles to energy conversion and initial SOC of the battery (SOC_t^i). It is assumed that the information about EV battery's SOH and SOC is obtained from the on-board battery management system (BMS). However, miles to energy conversion vary based on type of EV (which may be determined) and driving and weather conditions (which are difficult to determine). The road, weather, and traffic conditions are not considered in the controller formulation. However, allowance may be made through estimation or based on forecasting.

The first step in translating user demand is to convert the commanded target miles to corresponding amount of watt-hour (Wh) energy using the energy conversion coefficient. This coefficient is affected by several factors such as driving behaviour, loading profile, road conditions, and temperature. For this work, the official average energy consumption of Nissan LEAF ($220\,\mathrm{Wh/mile}$) tested for New European Driving Cycle (NEDC) is used as a reference for EV loading. However, the controller is adaptable to conversion factors from other manufacturers (such as from Tesla, BMW, Ford) and driving conditions and performs the necessary miles to Wh energy conversion. Once the required energy is obtained, the next step is converting it to equivalent SOC required by EV battery (SOC_t^r) for delivering specified miles. Thus, a lookup table has been used, which accurately determines the relative SOC based on battery energy capacity and SOH (determined by the number of charging cycles). The relationship between battery SOC, p.u. of battery capacity and cycle number is graphically shown in Fig. 4. The p.u. energy capacity would help in generalizing the proposed method for a battery of any capacity. The energy storage capacity of battery decreases when it is cycled (aged) and so is the SOH. To this end, cycle number (charge/discharge) gives a good estimation of the SOH. When the cycle number becomes high, the battery energy storage

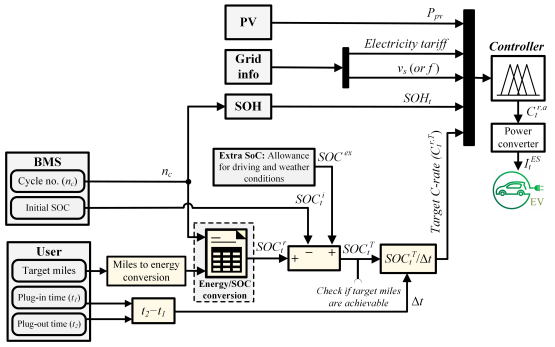

Fig. 3. Schematic diagram for implementation of smart charge controller.

capacity decreases and it may not be able to provide the maximum miles desired by the user. Thus, the proposed smart controller allows for the aging of the battery.

Fig. 4, shows that the same amount of energy requires different SOC levels for different SOH (cycle number, n_c). The graph depicts upper limit on the battery energy-storage capacity in case of higher cycle number (more degradation). As n_c increases, the battery energy storage capacity decreases (i.e. it cannot store as much energy as when new). Once, the desired SOC is determined with respect to energy and cycle number, an extra 10% SOC (SOC^{ex}) is added as an allowance for driving and weather conditions so as to ensure battery should not discharge to zero (to help protect the battery health), and a target SOC (SOC_t^T) is calculated as in (1).

$$SOC_t^T = SOC_t^r + SOC^{ex} - SOC_t^i \tag{1}$$

where, SOC_t^T, SOC_t^r, SOC^{ex} and SOC_t^i are target, required, extra and initial SOCs, respectively.

Note that the controller has the capability to take user required SOC as an input and in that case the mile to energy conversion step is disregarded and the target SOC is calculated directly using (1). For example, if the user during the stay period requires to charge battery to full, the required SOC can be set to 100%, which then be followed by controller to ensure the delivery of charging rate based on controller inputs. The target SOC, SOC_t^T (containing the count from required, initial and extra 10% SOCs), is further analysed by the controller to check if target miles are achievable (in other words, it is checked that if the SOC_t^T is less than 100%) and if not, the user will be notified. Finally, the waiting time (Δt) is used to calculate the target *C-rate* ($C_t^{r,T}$), given in (2). The *C-rate* is often used to describe the battery charging current rate (nC means the current in amps equals n times the capacity in ampere-hours). The higher or lower charging rate can be achieved by rapid ($1\,\mathrm{h}$) or slow domestic ($8\,\mathrm{h}$) charging.

$$C_t^{r,T} = \frac{S_t^T}{\Delta t}, \qquad 0.125C \leq C_t^{r,T} \leq 1C \tag{2}$$

where, waiting time $\Delta t = t_2 - t_1$ with t_1 and t_2 representing the plug-in and plug-out time in hour (h), respectively.

B. Battery state-of-health

Battery current SOC and SOH are important factors to consider and thus it is important to consider these for controller's formulation. The SOC is defined as the percentage of the maximum possible charge present in a battery. The SOH reflects the general condition of a battery and its ability to

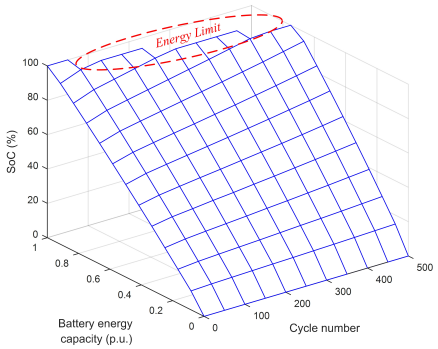

Fig. 4. Relationship between battery SOC (%), energy capacity (p.u.) and cycle number (n_c).

deliver usable capacity in comparison to a healthy battery [17]. In this paper, the battery SOH is described as the difference between the usable capacity and the end of life capacity (usually 80% of the rated capacity [35]) as a percentage of the rated (fresh) capacity. The on-board battery-monitoring unit provides the current SOC and total number of charge/discharge cycles to the algorithm. The proposed controller calculates the amount of energy present in the battery and SOH based on information received. Assuming the usable capacity of a healthy battery is 100%, the SOH can be defined as in (3).

$$SOH = 100\% - 80\% - f(n_c) \tag{3}$$

where, $f(n_c)$ is a function of cycle number. For a healthy battery $f(n_c) = 0$, and for a battery nearly towards the end of EV life, it holds a value of 20%, thus, SOH would stay in limits of 0 to 20%.

C. RES specifications

The controller requires output power from RES (PV) system in order to control the charging current in response to RES generation, thus EV charges from RES and responds to its intermittency. Renewable (PV) generation may be monitored in either real-time (perhaps locally) or forecasted based on weather information from the met office. The fault on the PV system is measured from the output PV power. The controller directly manages the increase or decrease in the PV production by accordingly changing the charging rate. The control algorithm is designed for per-unit value of RES (PV) power (this offers modular and scalability feature in the design).

D. Grid information

The grid information including grid voltage, frequency, (dynamic) tariff, main feeder current, etc. may be communicated by the distribution system operator (DSO) or an aggregator to the smart controller via the smart meter as shown in Fig. 2. Alternatively, grid local information as measured by smart meter may be used, e.g. voltage, current or frequency. The controller needs basic communication with the electric utility to receive the electricity price signal every $1h$. In this paper, the grid voltage (in p.u.) and tariff (in p.u.) are considered as inputs for the operation of smart controller. The lower and upper grid voltage limits are considered as -6% and $+10\%$, respectively, i.e., $0.94\,p.u.$ (min.) and 1.1 p.u. (max.). The controller is designed based on these statutory voltage limits which direct it to intelligently respond to any variations occurring in the grid (faults etc.) so as to provide grid support by adaptively controlling the charging rate, thereby reducing the negative impact of EV restricting it from further affecting the grid.

E. Controller output (C-rate)

To summarize, the inputs to the Fuzzy system are PV power (P_t^{pv}), grid information (voltage and tariff), battery initial SOC and SOH information provided by the BMS, and $C_t^{r,T}$ as function of EV user input data. In response to these inputs, the proposed controller generates the actual charging rate signal ($C_t^{r,a}$), which drives the power converter that charges the EV battery, as shown in Fig. 1. Various EV charging ranges are available for Nissan Leaf battery, such as, such as, the rating for slow charger is 3 kW (requires 14 h to fully charge battery from 0% SOC), 6.6 kW for fast charging (requires 6 hours to fully charge) and 50 kW for rapid charging (requires 40 mins to charge from 0 to 80%). Consequently, the Nissan leaf has the capability to be charged fast with 6.6 kW or rapid charging with 50 kW. The proposed controller suggests adaptive charging that will vary according to considered control parameters, one of them is the required SOC and waiting time. Thus, the power electronic converter must be capable of providing the required charging reference provided by the proposed smart charge algorithm. For 40 kWh Nissan leaf battery, the rated charger power for 1C operation must be at least 40 kW (i.e., charging EV with 1 C for a period of 1 h and reaching from 0 to 100% SOC). Thus, as per available charging range of Nissan Leaf it is suggested that the power electronic converter must have a power handling capability of 50 kW with full control over the injection of provided reference charging rate.

The actual charging current fed to the battery (in amperes) is determined by multiplying the controller generated charging rate ($C_t^{r,a}$) by the usable capacity ($\grave{U}_t$) of battery (which is defined as function of battery's SOH, in other words n_c). For example, the equivalent cell capacity for a healthy Nissan LEAF is 66 Ah. Thus, the maximum charging current at 1 C is 66 A. For a "nearly dead" battery ($\grave{U}_t$ is 80%) and thus, 1 C is $66\,\text{A} \times 80\% = 52.86\,\text{A}$. Thus, the amount of current (I_t^{ES}) delivered to battery by power converter is defined as:

$$I_t^{ES} = C_t^{r,a} \times \grave{U}_t(n_c), 80\% \leq \grave{U}_t \leq 100\%, \infty \geq n_c \geq 0 \tag{4}$$

III. The Proposed Smart Charge Controller

Smart chargers developed using rules based simple Fuzzy logic controller provide desired response based on inputs and pre-defined rules. The downside is that they require efforts in defining the rules and become complex in terms of implementation if the number of inputs to the system increases. To reduce complexity, a Neuro-Fuzzy controller is used in this work, which significantly reduces the number of rules while achieving satisfactory performance. To optimize the controller response, Particle Swarm Optimization (PSO) has been introduced, where based on a specific pre-defined cost function, controller's performance is enhanced and optimized. The PSO achieves optimal output taking into account user

profit and target charging rate, but it is computationally very demanding. Thus, PSO is combined with neural network and a Neuro-Fuzzy PSO is proposed to provide an intelligent and simple to implement optimized smart charge controller.

A. Rules based Simple Fuzzy (SF)

Fuzzy logic controller works on the principle of rules, designed and applied to the inputs during the Fuzzification process and generates the output while considering the pre-defined logic incorporated within the rules [36]. The Fuzzification process mainly involves deciding appropriate membership functions (mfs) and the choice of mfs shape affect the translation of crisp (original) inputs to Fuzzy values and the overall Fuzzification. Numerous commonly used mfs exist in the literature such as trapezoidal, triangular and Gaussian etc. However, considering the properties of chosen inputs and outputs, in this paper, a combination of triangular and trapezoidal mfs are used. The Defuzzification stage also involves membership function and the method used is 'centroid'. The definition of rules with respect to each input require feasible ranges in which inputs may vary.

A graphical representation of input limits for voltage, PV, SOH and tariff is presented in Fig. 5. Trapezoidal type membership function is employed for voltage, PV and tariff, whereas triangular mf is used for the target $C_t^{r,T}$. The voltage rules are defined using three trapezoidal mfs for low, normal and high voltage values (where the ranges are identified as 0.94 to 0.98 p.u. for low, 0.98 to 1.06 p.u. for normal and 1.06 to 1.1 p.u. for high). Likewise, the p.u. tariff falls in three ranges, low (0.3 to 0.55), medium (0.55 to 0.65) and high (0.65 to 1). The ranges for PV trapezoidal mfs are 0 to 0.2 p.u. for low, 0.4 to 0.6 p.u. for medium and 0.6 to 1.0 p.u. for high generation. The algorithm considers SOH using poor (0 to 0.07), normal (0.07 to 0.13) and healthy (0.13 to 0.2) membership functions. Finally, $C_t^{r,T}$ is incorporated as input using the triangular membership functions ranging from very low (VL) to Extremely High (EH) with ranges marked in Fig. 5 (e). As an example, under faulty grid conditions, if the grid voltage falls below the minimum threshold, the controller turns the Extremely Low mode for charging and on the other hand, a high voltage triggers the Extremely High charging mode, compensating thus for grid faults. The performance of simple Fuzzy (SF) has been verified for realistic case studies in Section IV, where it is shown that SF generates required *C-rate* in agreement to the pre-defined rules and follows variations in inputs.

The downside of SF is that it requires effort in defining rules and becomes complex in terms of implementation if the number of inputs to the system increases. It is important to note that with three inputs (having three mfs each) to Fuzzy system, the number of rules are 55. By adding fourth input, rules are increased to 163 and subsequently, they reach 487 when considering a fifth input. So, by adding another input with at least three membership functions, the number of rules will increase to 1459. Thus, increasing further the inputs, the rules continue to increase. In general, to add a new input with "n" number of membership functions, the number of existing rules multiplies by "n"; thus significant time and efforts to redefine the rules and apply them to the system.

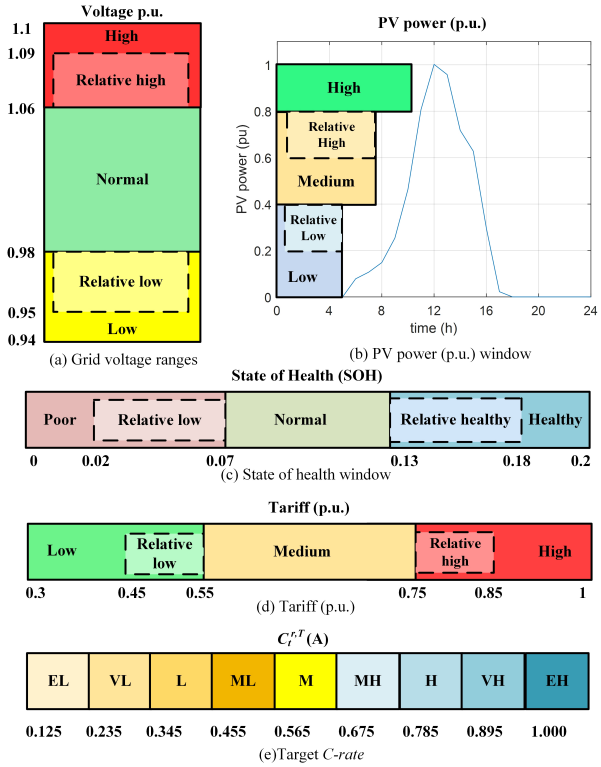

Fig. 5. Fuzzy rule windows for grid voltage, PV power, SOH, tariff and $C_t^{r,T}$. Note: Low (L), Extremely (E), Medium (M), High (H), Very (V).

B. Neural Network based Fuzzy (Neuro-Fuzzy)

For simple Fuzzy, number of rules increase with increasing inputs, achieving in this way a system with desirable specifications. However, increasing the number of rules each time for a new input is a difficult process, increasing the implementation complexity and requires exhaustive efforts. Neural network has been used to solve the problem of increasing number of inputs and so the rules. The flow diagram of the proposed Neuro-Fuzzy method is illustrated in Fig. 6. Assume that the simple Fuzzy with 163 rules is available and is able to provide $C_t^{r,a}$ corresponding to four-input (voltage, SOH, $C_t^{r,T}$, and PV). The first step is to train the Neural Network based on the input and output of four-input simple Fuzzy. Following this, a new input can be add to the system by setting a fewer number of rules in the Fuzzy logic (step 3). This can be continued for higher number of inputs easily with lesser number of rules in comparison to simple Fuzzy. For a six-input system, at least 1459 rules needed for simple fuzzy method. In contrast, only 27 rules need to be defined under the proposed Neuro-Fuzzy schematic with a pre-trained 5-input network. A comparison of SF and NF based on rules in the training and implementation is provided in Table II, where, a significant reduction in rules and implementation complexity is observed for NeF.

A generic structure of Neural Network is shown in Fig. 7. This structure has four hidden layers with variable number of neurons. The number of neurons in the hidden layers are considered variable to achieve minimum mean square error (MSE). If the MSE is not less than set limit, the neural network is retrained with the new number of neurons. After a couple of

TABLE II
COMPARISON OF SF AND NEF BASED ON RULES REQUIRED IN TRAINING AND IMPLEMENTATION STAGES.

Controller type→ Inputs↓	Simple Fuzzy rules	Neuro-Fuzzy rules	
	Implementation	Training	Implementation
4	163	163	0
5	487	163	27
6	1459	163	81

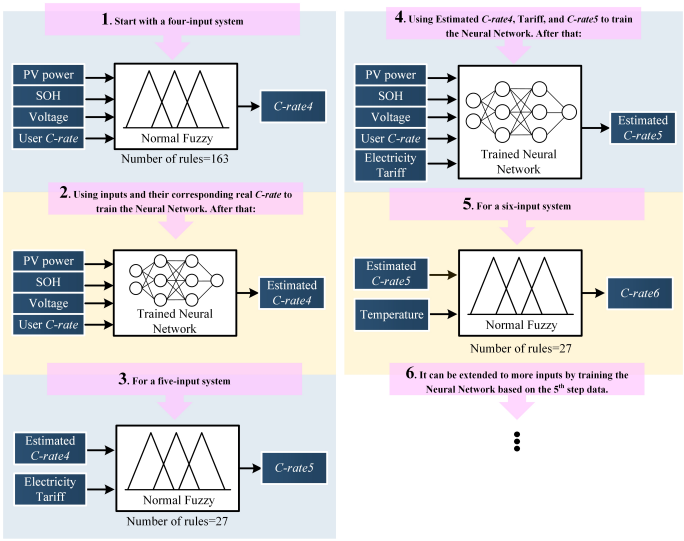

Fig. 6. Equivalence of N-input system based on proposed Neuro-Fuzzy method.

training, it has been realized that the ideal number of hidden layers in the understudy system are 4. With a mean square error of $6.4e^{-04}$ of the test data, the number of neurons in layers 1-4 are 11, 12, 14, and 22, respectively. Alongside, weight and bias values are updated according to the conjugate gradient backpropagation (*traincgp*) training function.

This method takes benefits of simple Fuzzy and overcomes its weakness related to increasing number of rules. In general, this method is suitable for replacing the methods and algorithms having low speed in online implementation such as Fuzzy Q-learning or the methods whose implementation becomes more complicated with increasing number of inputs. The neural network solves the problem of large number of rules as it was in the case of Simple Fuzzy. The neural network is achieving output in a closer agreement to simple Fuzzy but is not yet optimized. Thus, Particle Swarm Optimization (PSO) technique has been introduced. The main objective would be optimizing a cost function chosen to target optimizing specific variable or system parameter.

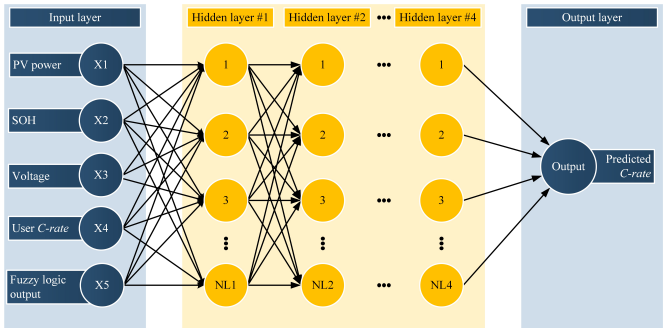

Fig. 7. Structure of neural network with several inputs and hidden layers.

C. Fuzzy Particle Swarm Optimization (Fuzzy-PSO)

Simple Fuzzy is intelligent and responsive to system variations but is demanding in term of defining rules, whereas Neuro-Fuzzy provides reduced complexity in terms of lesser rules required for implementation. The optimized feature is added to controller's output using PSO. In other words, simple Fuzzy or Neuro-Fuzzy is considered as an open-loop system, and thus, combining it with the PSO results in a closed-loop system giving optimal controllability over the generated *C-rate*. PSO changes the intervals of membership functions under fixed rules seeking a suitable output from fuzzy logic that leads to an improvement to the system. Thus, by determining suitable objective function, system specifications can be monitored and a more appropriate output of fuzzy logic can be obtained according to given set of rules. More specifically, optimization algorithm is involved in determining the ranges for membership functions by considering their points as input variables (where only the range of each membership function changes). It rearranges the membership function based on defined optimization problem. Under a proper multi-objective function, the membership functions (for inputs and output) are rearranged to achieve the optimum actual *C-rate*. An example of multi-objective function [37] is as follow:

$$\begin{aligned}\text{Min}(\pi_t^{tot}) = \text{Min}\Big[&(E_t^{GR+} \times \pi_t^{GR+}) \\ &-(E_t^{GR-} \times \pi_t^{GR-}) + \big(\tfrac{\pi_t^{ES}}{\alpha_h} \times (100 - SOH_t)\big)\Big]\end{aligned} \tag{5}$$

where, π_t^{tot} is total operating cost of system (in £) for time t, E_t^{GR+} is energy purchased from utility grid (kWh), E_t^{GR-} is energy feed-in to utility grid (kWh), π_t^{GR+} is purchasing power tariff (£/kWh), and π_t^{GR-} is feed-in power tariff (£/kWh). Likewise, π_t^{ES} is energy storage (battery) cost (£/kWh), SOH_t is the battery SOH and α_h is SOH constant reflecting the maximum SOH limit (holding a value of 20%).

At each time step t, a random value of variable matrix is formed. The column and row in the variable matrix indicate the number of optimization variables (n) and particles (m), respectively. Optimization variables in this case are the points from Fuzzy Logic membership functions, whereas, each particle consists of two parts, position (x) and velocity (v). At the beginning of algorithm, assuming that the best position is the same random value of variable matrix, membership functions corresponding to each particle is formed and value of *C-rate* is calculated. Therefore, considering actual current of battery I_t^{ES} in (4), excess power P_t^{Ex} in (6), the objective function (OF) can be obtained based on the value of *C-rate*.

$$P_t^{Ex} = \underbrace{P_t^{pv} \times \bar{P}^{pv}}_{Generation} - \underbrace{I_t^{ES} \times V_t^{ES}}_{Consumption} \tag{6}$$

where, P_t^{pv} is PV power in p.u.. at time t and $\bar{P}^{pv}$ is the maximum PV system capacity, I_t^{ES} is the energy storage current calculated using (4) and V_t^{ES} is the voltage.

The first and important step is to identify target variables and develop the objective function. The objective involves maximizing output *C-rate* and/or financial profit, thus, it is

important to include both in the formulation of objective function for the optimization problem. To show the significance of PSO, three objective functions (OF1, OF2, or OF3) have been defined in (7), (8) and (9), respectively. The OF1 aims at maximizing *C-rate* ($C_t^{r,a}$) only, OF2 maximizes the financial profit (f_t^p), whereas OF3 achieves a tradeoff while trying to maximize both *C-rate* and f_t^p.

$$max\left(C_t^{r,a}\right) = \frac{1}{C_t^{r,a}} \tag{7}$$

$$max\left(f_t^p\right) = \begin{cases} \frac{1}{P_t^{Ex}}, & P_t^{Ex} > 0 \\ -P_t^{Ex}, & P_t^{Ex} < 0 \end{cases} \tag{8}$$

When surplus power $P_t^{Ex} > 0$, the objective is to maximize the sold power. In contrast, when $P_t^{Ex} < 0$, minimization of power purchased from the utility grid is the primary objective. The OF3 combines the maximization of both *C-rate* and financial profit with a tradeoff of between the two.

$$max\left(C_t^{r,a}, f_t^p\right) = \begin{cases} \frac{w_{11}}{C_t^{r,a}} + \frac{w_{12}}{P_t^{Ex}}, & P_t^{Ex} > 0 \\ \frac{w_{21}}{C_t^{r,a}} - w_{22} \times P_t^{Ex}, & P_t^{Ex} < 0 \end{cases} \tag{9}$$

The tradeoff between *C-rate* ($C_t^{r,a}$) and profit maximization is determined by weighting factors ($w's$), which are optimized to achieve suitable tradeoff. An analysis shows that w_{12} has the most impact on the results.

The PSO algorithm stores set of variables that result least value in comparison with the other set called the best position (x^{id}). In addition, each particle belongs to a neighborhood (p^{id}), and thus, its movement (velocity, v) toward the optimal position (x) is influenced by the best experience of particles within this locality. Thus, for iteration $t+1$, the velocity and position of particle within a neighborhood is given by (10) and (11), respectively.

$$v_{t+1}^{id} = \omega v_t^{id} + c_1 r_1 \left(p^{id} - x_t^{id}\right) + c_2 r_2 \left(p^{id} - x_t^{id}\right) \tag{10}$$

$$x_{t+1}^{id} = x_t^{id} + v_{t+1}^{id} \tag{11}$$

where, $i = 1, 2 \ldots m$, $d = 1, 2 \ldots n$, $\omega =$ inertia weight, c_1 and c_2 are two positive acceleration parameters, called social and cognitive parameter, respectively, and r_1 and r_2 are random numbers uniformly distributed between $(0, 1)$.

At the beginning of algorithm, the best position is assumed as the same random value of variable matrix. Thereafter, particle position updates continuously until the pre-defined converging criteria is satisfied. The optimization stop criterion is set as either the number of iterations reaches the maximum or the objective function is less than the set value. After each update, Fuzzy Logic calculates *C-rate* based on the new position of particles. As the position of particles changes, so the way forming the membership functions and consequently the *C-rate*. The advantage of combining PSO with Fuzzy Logic is that these changes are applied in a way that leads to maximizing cost function and achieving desired objective.

A detailed flow diagram for Fuzzy-PSO algorithm is presented in Fig. 8 (movement from "*a*" to "*i*") and stepwise execution is explained as:

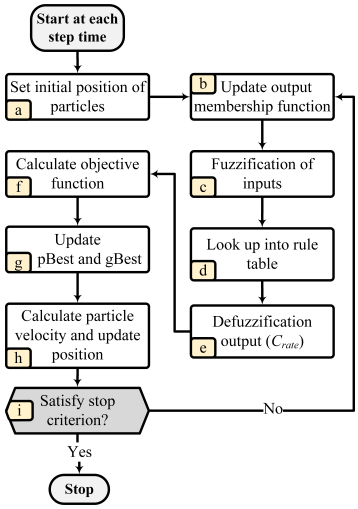

Fig. 8. Flow chart for the execution of proposed PSO.

a) Optimization variables are determined randomly and serves as formation for output membership function.
b) Given the selected input variables, output membership function is formed.
c) Fuzzification of inputs according to their respective membership functions. For example, for PV, convert "0.9 p.u." to "High" and so on for the other inputs (such as tariff, voltage etc.).
d) Finding output of Fuzzy logic controller based on the set rules.
e) Defuzzification of the output (converting the Fuzzy logic output to a real/crisp value) based on output membership function.
f) Calculating the objective function based on $C_t^{r,a}$ and financial profit, using (7), (8) or (9).
g) Finding best experience for individual and group of particles.
h) Updating particles characteristics, velocity (v) and position (x) using (10) and (11), respectively.
i) Check for stopping criterion, if the number of iterations reaches the quorum or the minimum value of the objective function is lower than the specified limit, the algorithm stops.

In the end, setting up *C-rate* related to the lowest value of objective function as the output for that time step.

D. Neuro Fuzzy Particle Swarm Optimization (NeFPSO)

The proposition of PSO optimizes the charging rate and enhances further the overall performance of smart controller. However, a significant disadvantage of PSO is the processing time, which require exhaustive efforts from controller and presents a challenge to the processor of embedded microcontroller. Furthermore, FPSO is accompanied by undesirable variations and chattering under constant input signals. This is due to reason that at each time step, the PSO algorithm starts with a random set of variables in a limited space and obtains the minimum value of the cost function after several specified iterations. Hence, when the inputs are constant for several time steps, the optimization output may be accompanied by a small

variation due to this random limited process. Consequently, to overcome these problems while maintaining the optimized performance, a Neural Network (presented in subsection III-B) is combined here with Fuzzy-PSO forming a new controller named as Neuro-Fuzzy PSO (NeFPSO). In, NeFPSO method, neural network is trained based on a large number of input datasets and their corresponding outputs. Although, the controller output corresponding to each input dataset is obtained from the PSO algorithm but it is unique. This is because the optimization is enabled only once for each input set. In the training step, only one output is predicted for each input set. Therefore, after the training, if the algorithm runs for fixed inputs in different time steps, the output of NeFPSO algorithm will be unique, thus presents robustness to random nature of PSO while still maintaining the optimization goals.

To emphasize the formulation of controller, a single-hidden-layer feed forward neural network is used in the proposed smart controller, presented in Fig. (9) and expressed as in (12).

$$N_i = \sum_{j=1}^{R} \left(Iw_{i,j} x_j + Hb_i \right), \forall i = 1, 2, ..., n \tag{12}$$

$$H_{Oi} = f\left(N_i\right), \forall i = 1, 2, ..., n \tag{13}$$

$$y = \sum_{j=1}^{n} \left(Hw_i Ho_i + Ob \right) \tag{14}$$

where, R and n are respectively the number of input and hidden nodes, Iw and Hw are the input and hidden weights matrices, respectively, Hb is the bias vector of the hidden layer, Ob is the bias value of the output layer, x is the input vector of the network, Ho is the output vector of the hidden layer, and y is the network output. Various forms are possible for the sigmoid function, f. A commonly used form is:

$$f\left(N_i\right) = \frac{2}{\left(1 + e^{-2N_i}\right) - 1} \tag{15}$$

To have an accurate trained neural network (TNN), variables such as, Iw, Hw, Hb, and Ob should be adjusted to minimize an error function, F, such as sum of squared errors (SSE) between network output, y^k, and desired target, T^k, as:

$$F = \sum_{k=1}^{m} e_k^2 = \sum_{k=1}^{m} \left(T^k - y^k \right)^2 \tag{16}$$

where, m is number of input-target (XT) sets for neural network training and the input ranges are shown in Fig. 5.

For a given l number of inputs, $XT_{m,l}$ sets can be generated by applying different input sets ($X_{m,l}$) to fuzzy logic.

$$X_{m,l} = \begin{bmatrix} x_{11} & x_{12} & \cdots & x_{1l} \\ x_{21} & x_{22} & \cdots & x_{2l} \\ \vdots & \vdots & \cdots & \vdots \\ x_{m1} & x_{m2} & \cdots & x_{ml} \end{bmatrix} \tag{17}$$

$$T_{m,l} = SF_1(X_{m,l}) \tag{18}$$

$$XT_{m,l} = \begin{bmatrix} X_{m,l} & T_{m,l} \end{bmatrix} \tag{19}$$

where, l is the number of inputs and SF_l is normal fuzzy operator for l-inputs. This way, neural network will be trained for l number of inputs (NN_l) which can be used as a substitution of the SF_l whenever the number of inputs are increased. For instance, for l+1 number of inputs, there is no need to define large number of rules for simple fuzzy with l+1 number of inputs (SF_{l+1}). This arrangement of controller leads to save time and reduce the complexity.

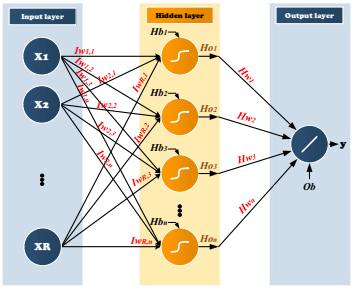

Fig. 9. Single-hidden-layer feed-forward neural network with one output.

$$SF_{l+1}\left(X_{m,l+1}\right) \cong SF_{l+1}^{NN_l}\left[NN_l(X_{m,l}) \quad x_{m,l}^{(l+1)} \right] \tag{20}$$

where, $x_{m,l}^{(l+1)}$ is a set of the input l+1 and $SF_{l+1}^{NN_l}$ is the SF with NN_l as lumped input. Assuming that each input has MF number of membership functions, $SF_{l+1}^{NN_l}$ will have $MF^l \times (MF-1)$ number of less rules than SF_{l+1}. To further increase the number of inputs to as l+2, neural networks must be re-trained as follows:

$$X_{m,2}^{(l+2)} = \left[SF_{l+1}^{NN_l}\left[NN_l(X_{m,l}) \quad x_{m,l}^{(l+1)} \right] \quad x_{m,l}^{(l+2)} \right] \tag{21}$$

$$T_{m,l}^{(l+2)} = SF_{l+2}^{NN_{l+1}}\left(X_{m,2}^{(l+2)} \right) \tag{22}$$

$$XT_{m,l+2} = \left[X_{m,2}^{(l+2)} \quad T_{m,l}^{l+2} \right] \tag{23}$$

where $x_{m,1}^{(l+2)}$ is a set of the input l+2, $X_{m,2}^{(l+2)}$ is a reduced-number of l+2 input sets, and $SF_{l+2}^{NN_{l+1}}$ is the SF with $SF_{l+1}^{NN_l}$ as lumped input. According to (20) and (22), each time an input is added, it is required to set new rules only for two inputs. This procedure dramatically increases the controller compatibility, especially in real-time optimizations. The optimal scheduling is time consuming process and is typically used offline. Fuzzy logic output can be obtained using an optimal approach, i.e., Fuzzy-PSO (flow chart for the execution of Fuzzy-PSO is illustrated in Fig. 8) and later used for the training of neural network based on the optimal results, giving rise to the proposed NeFPSO controller. In essence, Simple Fuzzy is intelligent and responsive to system variations but is demanding in terms of defining rules, whereas Fuzzy-PSO is optimized but requires excessive processing requirements and undesirable variations for constant inputs. However, Neuro-Fuzzy PSO combines features and benefits from various controllers and serves as suitable candidate with intelligent and optimized response, and lower complexity.

IV. Results and Discussion

In this section, the proposed controllers have been tested for real field data (such as voltage, tariff and PV profiles) using MATLAB simulations and in real-time using dSPACE 1103 real-time digital simulator. The sampling rate of the controller is set to 10 kHz. The performance and significance of various developed algorithms are analysed based on accuracy (error indices, such as mean square error etc.)

and complexity (number of rules, processing times etc.). Note that this paper considers only one EV for the analysis as the proposed controlled is decentralized and modular and controls the operation and fulfill the requirements of individual users separately. This is one of the key benefits of the proposed controller as it considers the requirement from each individual user and accordingly control their charging rate given the network and battery conditions.

A. Simulation Results

The simulation work analyzes the performance of several controllers presented and prove the superior performance of NeFPSO incorporating the properties of the predecessor with an overwhelming advantage of lower complexity, processing time and improved performance. The data used for analysis is based on real voltage and tariff profiles, however, tariff data has been slightly modified to suit the scenarios of this paper having a PV source. Whereas, the PV data is obtained from renewable.ninja for Newcastle upon Tyne, UK. First the performance of simple Fuzzy and Fuzzy PSO is compared, which follows the comparison of FPSO to NeFPSO. The operation of smart charger using SF and FPSO is analyzed in response to varying grid voltage, PV power and electricity tariff with specific user requirements and battery health. The battery is considered healthy (cycled only once, $n_c = 1$) and user requires 86 miles to travel (where it is assumed that there is 20% initial SOC in the battery worth 18 miles of travel) and waiting time of user is 4 hours (plug-in at 1400 h, 0.0 h and 10.00 h).

The OF3 is of interest as it intends to fulfill two objectives (maximize *C-rate* and profit) useful to EV user while satisfying network and battery conditions. The variations in grid voltage, PV power and tariff are clearly reflected in the form of corresponding actual 10 and corresponding benefit in terms of financial profit and reduced charging time, given in Table III. The injection of PV (from 10 h to 16 h) increases net generation and voltage; thus, tariff reduces during this time. The variation in *C-rate* follows the changes in v, tariff and PV output. Thus, the developed controller is able to provide the actual *C-rate*, $C_t^{r,a}$, as set by the rules. In Fig. 10 (a), among three, FPSO performs economically and presents faster charging, whereas SF takes slightly more time and earns less profit. The uncontrolled charging, where *C-rate* is supplied based on user requirements (and without considering the other controller inputs) incur more cost (less profit) due to charging from grid during peak hours where tariff is high. The other two cases, user earn less profit due to reason that the objective for FPSO is maximizes *C-rate* and reduces the effective charging time with respect to uncontrolled charging. OF3 provides a reasonable trade-off, where in comparison to OF1, profit is increased and on the other hand, average C_rate presents higher value in comparison to OF2. An investigation shows that on average over 24-h, the increase in profit for OF3 in comparison to OF1 is 41.28%, whereas the increase in average C_rate for OF3 compared to OF2 is 5.92%. The OF3 is of interest as it intends to fulfill two objectives (C_rate and profit) useful to EV user while satisfying network and battery conditions.

TABLE III
ANALYSIS OF RESULTS FOR FUZZY-PSO FOR OF3.

	Fig. 10 (a)		Fig. 10 (b)		Fig. 10 (c)	
Controller↓	t^{chg}	$\tilde{f}_t^p$	t^{chg}	$\tilde{f}_t^p$	t^{chg}	$\tilde{f}_t^p$
SF	3.13	0.0403	2.17	-0.0195	2.12	0.0579
FPSO	2.75	0.0504	2	-0.0204	2.35	0.0573
No control	4	0.037	4	-0.0194	4	0.129

A significant disadvantage of PSO is the processing time, which require exhaustive efforts from controller and presents a challenge to the processor of embedded microcontroller. Furthermore, FPSO is accompanied by undesirable variations and chattering under constant input signals. Neural network has been used to solve the problem of increasing number of inputs (and so the rules) in the simple Fuzzy-based method and complexity for PSO. Consequently, Neuro-Fuzzy PSO (NeFPSO) overcome these problems while maintaining the optimized performance. A comparison of FPSO with NeFPSO is carried out for varying grid voltage, tariff, PV with battery condition ($nc = 1 \approx 0.199$ SOH) and user requirements (85 miles to travel with 40.12% initial SOC and 4 h waiting time). The corresponding results are graphically shown in Fig. 11 and summarized in Table IV. The performance accuracy of NeF can be measured using several indices Mean Absolute Error (MAE), Mean Absolute Percentage Error (MAPE), Mean Square Error (MSE) and Root Mean Square Error (RMSE). These indices are always positive and close to zero values is considered as ideal [38], [39]. The MAE calculates average significance of entire dataset giving equal weights to all errors of model, giving information about long-term accuracy. RMSE gives high weight to large errors, more useful when large errors are particularly undesirable, and thus robust in dealing with large deviations. The proposed NeFPSO tracks the reference *C-rate* generated by FPSO with a very good accuracy as can be verified from the MSE error of *Crate* and financial profit. It is worth mentioning that the accuracy is achieved with a very less computational complexity as measured from the processing time taken by the algorithm. FPSO require approximately 5 min 6 s for its processing, whereas the proposed NeFPSO takes 11 s only (approximately 2780% less time) for given user requirements, BMS measurements and network conditions. Thus, NeFPSO is responsive to network variations, presents intelligent, optimized and chattering-free response, considers renewable penetration and above all, possess very less computational complexity, emerging as an ideal solution for EV smart, less complex, optimized, user-, eco- and grid-friendly charging.

TABLE IV
PERFORMANCE EVALUATION OF FPSO AND NEFPSO UNDER OF3.

Index	FPSO	NeFPSO	MSE	Remarks
$\tilde{f}_t^p$	-0.0204	-0.0199	0.000187	FPSO requires 2780% more processing time
t_p	5 min 6 s	11 s	–	
t^{chg}	2 h	1.93 h	–	

To further present the analysis of various controllers and conclude the significance of proposed solution, a test case has been considered where the performance of controllers is examined over a period of 24 h. The 24 h case is considered to better reflect the impact of realistic voltage, tariff and PV profiles

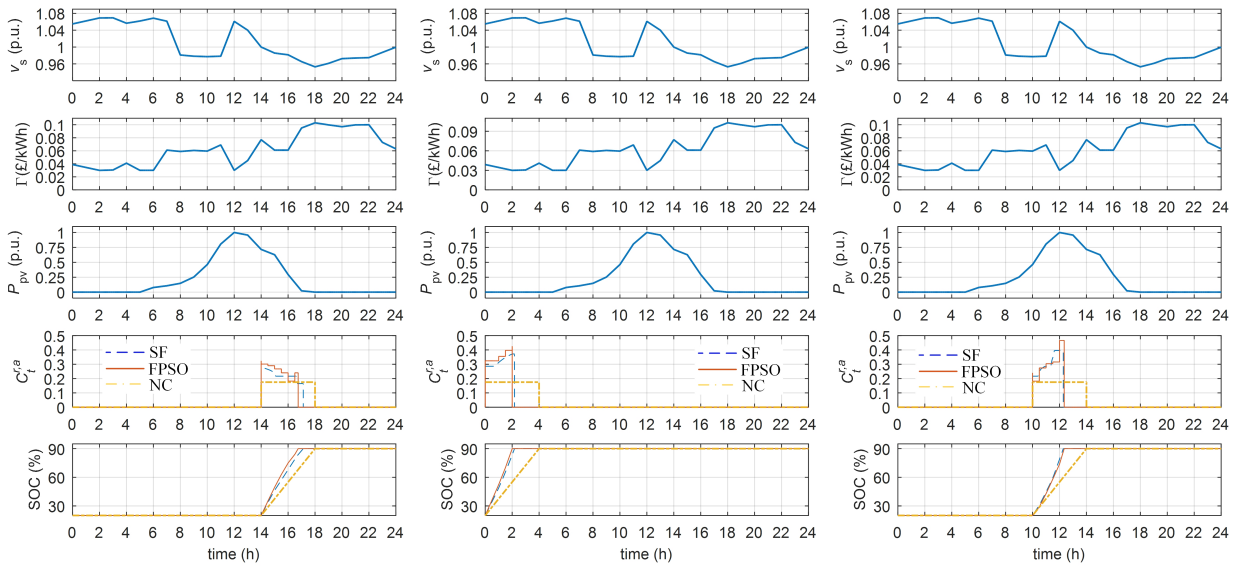

(a) Plug-in at 14.00 h (b) Plug-in at 0.0 h (c) Plug-in at 10.00

Fig. 10. The grid voltage, PV and tariff real variations and corresponding actual *C-rate*, $C_t^{r,a}$ for SF and FPSO.

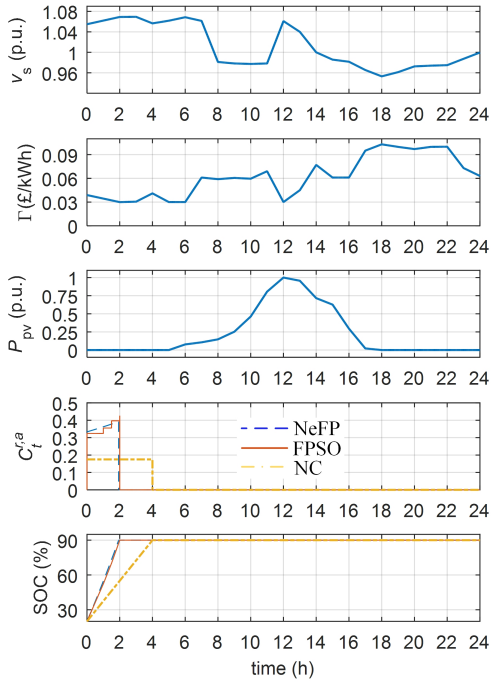

Fig. 11. Comparison of FPSO and NeFPSO under OF3.

on the controller output (measured as the average C_{rate} and financial profit). The performance indices considered are the financial profit and the mean of *C-rate*. The maximization of $C_t^{r,a}$ is observed and quantified using the mean of actual *C-rate* ($\overline{C_t^{r,a}}$) given in (24), whereas the mean of financial profit ($\overline{f_t^p}$) earned by user is calculated as in (25) as a function of system surplus power and energy tariff (Γ_t).

$$\overline{C_t^{r,a}} = \sum_{t_l=1}^{t_u=24} \left(\frac{C_t^{r,a}}{t_u} \right) \tag{24}$$

$$\overline{f_t^p} = \sum_{t_l=1}^{t_u=24} \left(\frac{\overbrace{P_t^{Ex} \times \Gamma_t}^{f_t^p}}{t_u} \right) \tag{25}$$

The test conditions are, the battery is considered as healthy (cycled only once, $n_c = 1$) and the user requires 85 miles to travel (where it is assumed that there is 42% initial SOC in the battery worth 40 miles of travel) and the waiting time of user is one hour. In this case, at first, the performance and significance of Fuzzy PSO is analyzed by comparing its response and performance to SF under three pre-defined objective functions (OF1, OF2 and OF3) for 24 h window, summarized in Table V and depicted in Fig. 11. It is important to mention that OF1 given in (7) aims at maximizing *C-rate* only, OF2 maximizes the financial profit (f_t^p), whereas OF3 achieves a trade-off while trying to maximize both *C-rate* and f_t^p.

The OF1 maximizes the $C_t^{r,a}$ while observing the constraints (such as the grid voltage, PV power and tariff) and the mean of *C-rate* is higher compared to SF, whereas the profit is reduced. Likewise, OF2 maximizes financial profit and compromise on $C_t^{r,a}$. The PSO optimal output from an economic or *C-rate* point of views depend only on the objective function. Consequently, OF3 provides a reasonable trade-off, where in comparison to OF1, profit is increased and on the other hand, $\overline{C_t^{r,a}}$ presents higher value in comparison to OF2. The increase in profit for OF3 in comparison to OF1 is 41.28%, whereas the increase in $\overline{C_t^{r,a}}$ for OF3 compared to OF2 is 5.92%. The OF3 is of interest as it intends to fulfill two objectives (*C-rate* and profit) useful to EV user while satisfying network and battery conditions.

Likewise, the FPSO under OF3 is compared with NeFPSO for 24 h window under same set of test conditions and results are presented in Table VI and Fig.12. A mean square error of 0.27% and 0.43% are observed in $\overline{C_t^{r,a}}$ and $\overline{f_t^p}$, respectively

which shows that the NeFPSO presents good tracking of the *C-rate* generated by FPSO. NeFPSO offer similar performance capabilities to FPSO but with lower complexity and faster processing, making it a suitable candidate for EV smart charging. Thus, on average (24 h) the use of proposed NeFPSO controller presents better performance and is beneficial for both EV and grid rather than the uncontrolled and simple Fuzzy based charging schemes.

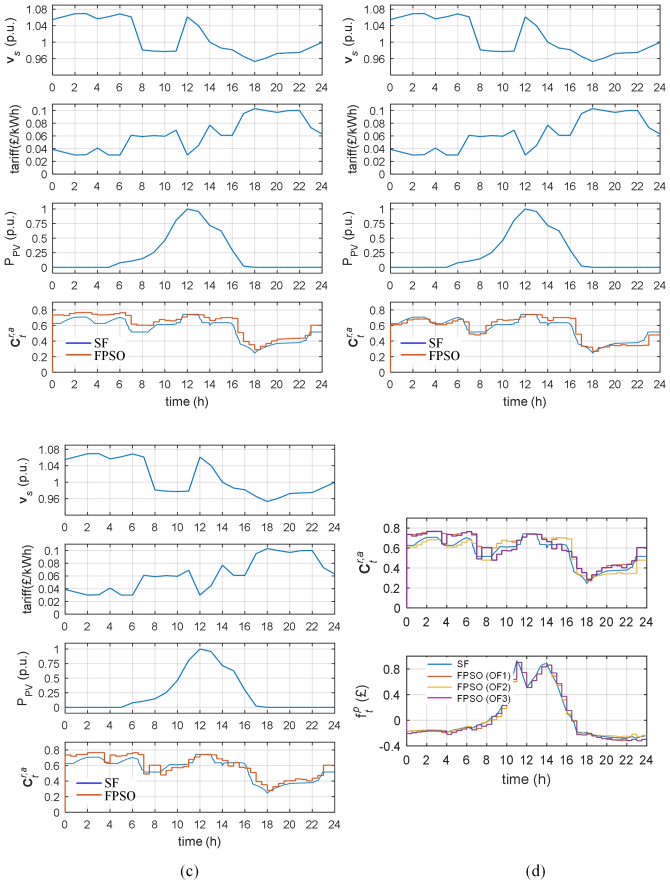

Fig. 12. (a) Comparison of SF and FPSO for OF1, OF2 and OF3, (b) Variation in profit over 24 h corresponding to $C_t^{r,a}$ for OF1, OF2 and OF3.

TABLE V
ANALYSIS OF FUZZY-PSO FOR RESULTS PRESENTED IN FIG. 11.

Objective function	$\overline{C_t^{r,a}}$	$\overline{f_t^p}$ (£)
FPSO OF1=$max(C_{rate})$	0.6204	0.0281
FPSO OF2=$max(f_t^p)$	0.5610	0.0535
FPSO OF3=$max(C_{rate}$ & $f_t^p)$	0.5942	0.0397
Simple Fuzzy	0.5563	0.0553

TABLE VI
PERFORMANCE EVALUATION OF FPSO AND NEFPSO UNDER OF3.

Performance index	FPSO	NeFPSO	MAE
$\overline{C_t^{r,a}}$	0.5442	0.5348	0.0027
$\overline{f_t^p}$	0.0620	0.0603	0.0043

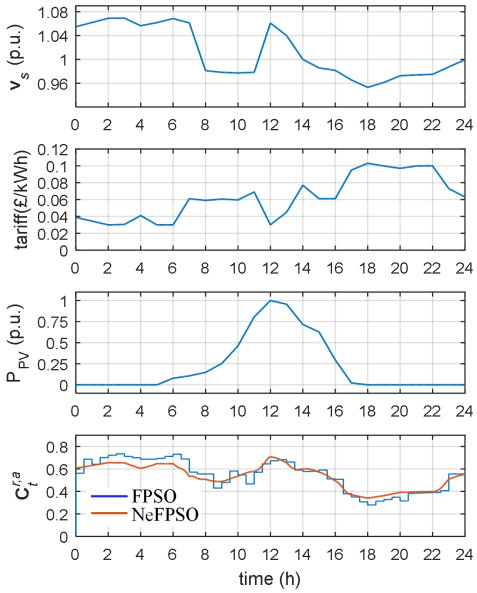

Fig. 13. Comparison of FPSO and NeFPSO for OF3.

B. Experimental Results

The real-time validation of proposed NeFPSO controller is carried out using dSPACE controldesk and MATLAB real-time interface. The user requires 85 miles to travel with 40.12% initial SOC and 4 h waiting time, battery condition (SOH = 0.199) and constant PV power of 0.75 p.u. The first case considers the impact of varying grid voltage on the output *C-rate*,presented in Fig. 14 *a*. The voltage is varied between 0.94 p.u. (min) to 1.06 p.u. (max) with fixed tariff of 0.008 £/kWh and the proposed controller's output *C-rate* clearly follows the variation and adjusts itself as per the increase and decrease in the grid voltage. Furthermore, controller is tested for variations in electricity tariff (Fig. 14 *b*) which are followed by controller and output *C-rate* is generated accordingly. These validations prove the real-time working and decision making of proposed NeFPSO towards grid support and tariff variations, fulfilling user requirements alongside keeping the constraints on SOH.

V. CONCLUSIONS

This paper proposes a Neuro-Fuzzy based novel and advanced smart charge controller for electric vehicle applications. The proposed controller optimizes EV charging rate in order to meet EV user requirements (waiting time and length of next trip) whilst considering EV battery state-of-health, local renewable energy (PV) generation, electricity tariff and grid condition (e.g. voltage or frequency level). Such controllers can have an important role in the design and control of future power networks (smart grid). The proposed Neuro-Fuzzy PSO provides accurate valuation of optimized charging rate and fast response with low computational complexity. Performance evaluation using realistic profiles and multiple indices (MSE, processing time and number of rules as measures of accuracy and computational complexity) validates the good performance of proposed controller for EV user requirements,

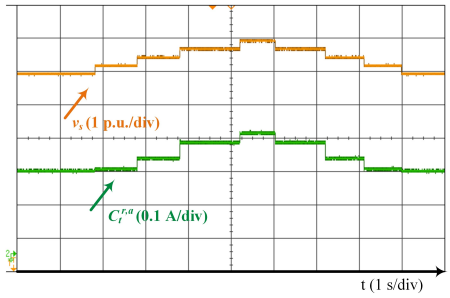

(a) Controller's response to varying grid voltage

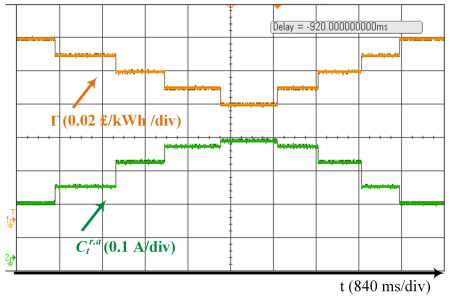

(b) Controller's response to varying electricity tariff

Fig. 14. Real-time validation of proposed NeFPSO smart charge controller.

BMS measurements, PV generation and network conditions. Thus, the proposed controller would help in improving the overall operation of smart grid by effectively responding to grid conditions and utilizing energy from RES while fulfilling user requirements.

REFERENCES

[1] D. for Transport, "Low carbon transport: a greener future, a carbon reduction strategy for transport, Report," July 2009. [Online]. Available: https://assets.publishing.service.gov.uk/government/uploads/system/uploads/attachment_data/file/228897/7682.pdf

[2] A. Mansour-Saatloo, Y. Pezhmani, M. A. Mirzaei, B. Mohammadi-Ivatloo, K. Zare, M. Marzband, and A. Anvari-Moghaddam, "Robust decentralized optimization of multi-microgrids integrated with power-to-x technologies," *Applied Energy*, vol. 304, p. 117635, 2021.

[3] H. Government, "Meeting the energy challenge: A white paper on energy," Department of Trade and Industry," Report, 2007. [Online]. Available: https://www.gov.uk/government/publications/meeting-the-energy-challenge-a-white-paper-on-energy

[4] F. Khosrojerdi, S. Taheri, H. Taheri, and E. Pouresmaeil, "Integration of electric vehicles into a smart power grid: A technical review," in *Proc. IEEE EPEC*, pp. 1–6.

[5] C. Zhang, F. Wen, G. Ledwich, and J. Lei, "Impacts of plug-in electric vehicles on distribution networks," in *Proc. IEEE IPEC*, pp. 115–120.

[6] B. Lunz, Z. Yan, J. B. Gerschler, and D. U. Sauer, "Influence of plug-in hybrid electric vehicle charging strategies on charging and battery degradation costs," *Energy Policy*, vol. 46, pp. 511–519, 2012.

[7] F. d. P. García-López, M. Barragán-Villarejo, and J. M. Maza-Ortega, "Grid-friendly integration of electric vehicle fast charging station based on multiterminal dc link," *International Journal of Electrical Power Energy Systems*, vol. 114, p. 105341, 2020.

[8] Y. Wang, S. Huang, and D. Infield, "Investigation of the potential for electric vehicles to support the domestic peak load," in *Proc. IEEE IEVC*, pp. 1–8.

[9] S. M. Kazemi-Razi, H. Askarian Abyaneh, H. Nafisi, Z. Ali, and M. Marzband, "Enhancement of flexibility in multi-energy microgrids considering voltage and congestion improvement: Robust thermal comfort against reserve calls," *Sustainable Cities and Society*, vol. 74, p. 103160, 2021.

[10] S. Zeynali, N. Nasiri, M. Marzband, and S. N. Ravadanegh, "A hybrid robust-stochastic framework for strategic scheduling of integrated wind farm and plug-in hybrid electric vehicle fleets," *Applied Energy*, vol. 300, p. 117432, 2021.

[11] N. B. M. Shariff, M. A. Essa, and L. Cipcigan, "Probabilistic analysis of electric vehicles charging load impact on residential distributions networks," in *Proc. IEEE ENERGYCON*, pp. 1–6.

[12] K. Clement-Nyns, E. Haesen, and J. Driesen, "The impact of charging plug-in hybrid electric vehicles on a residential distribution grid," *IEEE Trans. Power Systems*, vol. 25, no. 1, pp. 371–380, 2010.

[13] A. S. Masoum, S. Deilami, P. S. Moses, M. A. Masoum, and A. Abu-Siada, "Smart load management of plug-in electric vehicles in distribution and residential networks with charging stations for peak shaving and loss minimisation considering voltage regulation," *IET generation, transmission & distribution*, vol. 5, no. 8, pp. 877–888, 2011.

[14] S. Deilami, A. S. Masoum, P. S. Moses, and M. A. S. Masoum, "Real-time coordination of plug-in electric vehicle charging in smart grids to minimize power losses and improve voltage profile," *IEEE Trans. Smart Grid*, vol. 2, no. 3, pp. 456–467, 2011.

[15] M. Nour, S. M. Said, A. Ali, and C. Farkas, "Smart charging of electric vehicles according to electricity price," in *Proc. IEEE ITEC*, pp. 432–437.

[16] A. Neagoe-Stefana, M. Eremia, L. Toma, and A. Neagoe, "Impact of charging electric vehicles in residential network on the voltage profile using matlab," in *Proc. IEEE Symposium on ATEE*, pp. 787–791.

[17] R. M. Shukla, S. Sengupta, and A. N. Patra, "Smart plug-in electric vehicle charging to reduce electric load variation at a parking place," in *Proc. IEEE CCWC*, pp. 632–638.

[18] I. Sharma, C. Cañizares, and K. Bhattacharya, "Smart charging of pevs penetrating into residential distribution systems," *IEEE Trans. Smart Grid*, vol. 5, no. 3, pp. 1196–1209, 2014.

[19] B. Faridpak, M. Farrokhifar, A. Alahyari, and M. Marzband, "A mixed epistemic-aleatory stochastic framework for the optimal operation of hybrid fuel stations," *IEEE Transactions on Vehicular Technology*, vol. 70, no. 10, pp. 9764–9774, 2021.

[20] M. F. Shaaban, M. Ismail, E. F. El-Saadany, and W. Zhuang, "Real-time pev charging/discharging coordination in smart distribution systems," *IEEE Transactions on Smart Grid*, vol. 5, no. 4, pp. 1797–1807, 2014.

[21] M. Rahman, M. Othman, H. Mokhlis, M. Muhammad, and H. Bouchekara, "Optimal fixed charge–rate coordination of plug-in electric vehicle incorporating capacitor and oltc switching to minimize power loss and voltage deviation," *IEEJ Transactions on Electrical and Electronic Engineering*, 2017.

[22] M. Singh, P. Kumar, and I. Kar, "Implementation of vehicle to grid infrastructure using fuzzy logic controller," *IEEE Trans. Smart Grid*, vol. 3, no. 1, pp. 565–577, 2012.

[23] S. Pazouki, A. Mohsenzadeh, M. Haghifam, and S. Ardalan, "Simultaneous allocation of charging stations and capacitors in distribution networks improving voltage and power loss," *Canadian Journal of Electrical and Computer Engineering*, vol. 38, no. 2, pp. 100–105, 2015.

[24] C. O. Adika and L. Wang, "Smart charging and appliance scheduling approaches to demand side management," *International Journal of Electrical Power Energy Systems*, vol. 57, pp. 232–240, 2014.

[25] T. Jiang, G. Putrus, Z. Gao, M. Conti, S. McDonald, and G. Lacey, "Development of a decentralized smart charge controller for electric vehicles," *International Journal of Electrical Power Energy Systems*, vol. 61, pp. 355–370, 2014.

[26] A. Al-Obaidi, H. Khani, H. E. Z. Farag, and M. Mohamed, "Bidirectional smart charging of electric vehicles considering user preferences, peer to peer energy trade, and provision of grid ancillary services," *International Journal of Electrical Power Energy Systems*, vol. 124, p. 106353, 2021.

[27] K. Vinoth Kumar, P. Radhakrishnan, R. Kalaivani, V. Devadoss, L. D. Vijay Anand, and K. Vinodha, "Implementation of smart electric vehicle charging station driven using experimental investigation," in *Proc. IEEE GCAT*, 2021, pp. 1–5.

[28] M. Nour, S. M. Said, A. Ali, and C. Farkas, "Smart charging of electric vehicles according to electricity price," in *Proc. IEEE ITCE*, 2019, pp. 432–437.

[29] A. Shahkamrani, H. Askarian-abyaneh, H. Nafisi, and M. Marzband, "A framework for day-ahead optimal charging scheduling of electric vehicles providing route mapping: Kowloon case study," *Journal of Cleaner Production*, vol. 307, p. 127297, 2021.

[30] M. H. Mobarak and J. Bauman, "Vehicle-directed smart charging strategies to mitigate the effect of long-range ev charging on distribution transformer aging," *IEEE Trans. Transportation Electrification*, vol. 5, no. 4, pp. 1097–1111, 2019.

[31] N. Gholizadeh, M. Abedi, H. Nafisi, M. Marzband, A. Loni, and G. A. Putrus, "Fair-optimal bilevel transactive energy management for community of microgrids," *IEEE Systems Journal*, pp. 1–11, 2021.

[32] S. Das, P. Acharjee, and A. Bhattacharya, "Charging scheduling of electric vehicle incorporating grid-to-vehicle and vehicle-to-grid technology considering in smart grid," *IEEE Trans. Industry Applications*, vol. 57, no. 2, pp. 1688–1702, 2021.

[33] M. S. Jonban, L. Romeral, A. Akbarimajd, Z. Ali, S. S. Ghazimirsaeid, M. Marzband, and G. Putrus, "Autonomous energy management system with self-healing capabilities for green buildings (microgrids)," *Journal of Building Engineering*, vol. 34, p. 101604, 2021.

[34] Z. J. Lee, G. Lee, T. Lee, C. Jin, R. Lee, Z. Low, D. Chang, C. Ortega, and S. H. Low, "Adaptive charging networks: a framework for smart electric vehicle charging," *IEEE Trans. Smart Grid*, vol. 12, no. 5, pp. 4339–4350, 2021.

[35] F. Marra, C. Træholt, E. Larsen, and Q. Wu, "Average behavior of battery-electric vehicles for distributed energy studies," in *Proc. IEEE PES ISGT Europe*, 2010, pp. 1–7.

[36] Y. Bai and D. Wang, "Fundamentals of fuzzy logic control—fuzzy sets, fuzzy rules and defuzzifications," in *Advanced fuzzy logic technologies in industrial applications*. Springer, 2006, pp. 17–36.

[37] Y.-S. Cheng, Y.-H. Liu, H. C. Hesse, M. Naumann, C. N. Truong, and A. Jossen, "A pso-optimized fuzzy logic control-based charging method for individual household battery storage systems within a community," *Energies*, vol. 11, no. 2, 2018.

[38] Ümit Ağbulut, A. E. Gürel, A. Ergün, and İlhan Ceylan, "Performance assessment of a v-trough photovoltaic system and prediction of power output with different machine learning algorithms," *Journal of Cleaner Production*, vol. 268, p. 122269, 2020.

[39] R. Ahmed, V. Sreeram, Y. Mishra, and M. Arif, "A review and evaluation of the state-of-the-art in pv solar power forecasting: Techniques and optimization," *Renewable and Sustainable Energy Reviews*, vol. 124, p. 109792, 2020.